

ORIGINAL ARTICLE

An investigation into structural behaviors of skulls chewing food in different occlusal relationships using FEM

Yeo-Kyeong Lee¹ | Youn-Sic Chun²

¹Architectural and Urban System Engineering, Division of Sustainable Systems Engineering, ELTEC College of Engineering, Ewha Womans University, Seoul, South Korea

²Orthodontics & dentofacial orthopedics, School of Medicine, Ewha Womans University, Seoul, South Korea

Correspondence

Hee-Sun Kim, Architectural and Urban System Engineering, Division of Sustainable Systems Engineering, ELTEC College of Engineering, Ewha Womans University, Seoul, South Korea. Email: hskim3@ewha.ac.kr

Jae-Yong Park, Architectural and Urban System Engineering, Division of Sustainable Systems Engineering, ELTEC College of Engineering, Ewha Womans University, Seoul, South Korea. Email: jypark1212@ewha.ac.kr

Funding information

the National Research Foundation of Korea (NRF) funded by the Ministry of Science, ICT & Future Planning, Grant/Award Numbers: NRF-2014R1A1A1007583, NRF-2017R1D1A1B03034274

Abstract

Objectives: This study aims to investigate the effect of different occlusal relationships on skull structural and mechanical behaviors through simulation of chewing food.

Methods: Finite element (FE) skull models of occlusion for Class I, end-on Class II, and full-cusp Class II were generated. End-on Class II and full-cusp Class II were chosen as mild and severe Class II occlusions, respectively. A simplified food bolus was introduced between the upper and lower dentition of the right molars. Chewing food was simulated in the skulls by moving the mandible. An experiment was conducted to measure strains at selective locations and compared them to the analytical results for validation.

Results: In the early stages of mandibular movement, masticatory forces predicted from the skull models without food were lower than the skull models with food but increased drastically after occluding teeth full enough. As a result, the relationship between masticatory force and mandible movement shows that there is no significant difference between the skull models with food and without food in the range of human masticatory force, approximately 250 N. In all the cases of skulls including a food bolus, stress was similarly propagated from the mandible to the maxilla and concentrated in the same regions, including the mandibular notch and alveolar bone around the lower molars.

Conclusion: It is predicted that there is no significant difference of bite force-mandible movement relationships and stress distributions of skull and teeth, between end-on Class II and full-cusp Class II models. When simulating chewing activities on candy and carrot, it is also found that there is no difference of masticatory performance between Class II occlusions, from structural as well as mechanical perspectives.

KEYWORDS

chewing simulation, FEA (finite element analysis), occlusal relationship, skull, structural behavior

1 | INTRODUCTION

According to the Korean Health Insurance Review & Assessment Service, orthodontic patients have been steadily increasing owing to

malocclusion treatment and aesthetic functions. During orthodontic treatment, extraction is generally done to retain teeth spacing and straighten teeth arrangement, which may cause changes of occluding and masticatory activities. Therefore, it is crucial to predict the

This is an open access article under the terms of the Creative Commons Attribution License, which permits use, distribution and reproduction in any medium, provided the original work is properly cited.

© 2020 The Authors. Clinical and Experimental Dental Research published by John Wiley & Sons Ltd.

differences in skull structural and mechanical behaviors according to different occlusal relationships.

Finite element (FE) analysis has been widely used to simulate different behaviors in dentofacial orthopedics and dental biomechanics (Ammar, Ngan, Crout, Mucino, & Mukdadi, 2011; Borcic et al., 2005; Cattaneo, Dalstra, & Melsen, 2005; Chang, Shin, & Baek, 2004; Field et al., 2009; Geramy & Morgano, 2004; Hsu, Chen, Chen, Huang, & Chang, 2009; Kibi et al., 2009; Lee, Choi, Lee, Ahn, & Noh, 2018; Liang, Rong, Lin, & Xud, 2009; Liu, Chang, Wong, & Liu, 2012; Rudolph, Willes, & Sameshima, 2001; Singh, Mogra, Shetty, Shetty, & Philip, 2012; Soares et al., 2014; Toms & Eberhardt, 2003; Vukicevic, Zelic, Jovicic, Djuric, & Filipovic, 2015; Yu, Baik, Sung, Kim, & Cho, 2007; Zhang, Cui, Lu, & Wang, 2017), because of many problematic issues in clinical testing, such as subject discomfort and limit of accessible areas. In the study conducted by Lee et al. (2018), FE analysis was performed to investigate the mechanical effect of different protrusion positions of a mandibular advancement device (MAD) on teeth and facial bones, since the MAD-induced stress and strain have not been measured directly from living structures. Ammar et al. (2011) used the FE jawbone model to simulate canine retraction with mini-screw anchorage and compared stresses on the mini-screw and fracture failure of tangential orthodontic forces. Zhang et al. (2017) constructed a mandibular first molar FE model and simulated various occlusal load conditions through area size, location, and direction of loading. Rudolph et al. (2001) and Cattaneo et al. (2005) also performed FE analyses of a 1 or 2 teeth model applying various orthodontic tooth movements and evaluating stress at the tooth, periodontal ligament (PDL), and alveolar bone. Liang et al. (2009) generated FE models of the maxilla and maxillary incisors and reported that teeth stress and strain distributions change depending on the orthodontic method; horizontal retraction force, intrusive vertical force, and lingual root torque. In the study conducted by Soares et al. (2014), the biomechanical behaviors of maxillary premolar teeth were estimated using FE analysis and strain gauge testing. They compared the predicted stress distributions regarding tooth root morphology and abfraction depth.

Relatively little research has been conducted to investigate occlusal behaviors from the full skull FE model. In the previous studies (Lee, Kim, & Park, 2017; Lee, Park, & Kim, 2016), FE modeling methods for simulation of occluding teeth in full-skull were proposed and parametric studies of boundary and loading conditions were performed through FE analysis to find out how to prescribe proper support and loading in the full skull model. Simulation is possibly much closer to actual activity using the full skull model, and the stress and strain distributions from the mandible to the maxilla can be predicted. Moreover, it can minimize the effect of modeling error, such as occlusal surface modeling, as one can investigate the structural behaviors of the skull from a more comprehensive overall viewpoint.

However, from a clinical viewpoint, it is imperative to know what happens mechanically in the skull and teeth when chewing food rather than just occlusion. Therefore, this paper aims to investigate the effect of different occlusal relationships on the structural and mechanical behaviors of skulls, such as forces and stress distributions through simulation of chewing food.

2 | MATERIALS AND METHODS

2.1 | Generation of FE model

CT images (SOMATOM™ SENSATION, Siemens AG, Germany, 120 kVp, 200 ms, 0.75 mm-thickness) were captured from a 38-year-old male skull with normal occlusion status and constructed as the FE skull model with a Class I occlusion (Figure 1); previously published papers detail the modeling process (Lee et al., 2016, 2017; Seol, 2014). Taking into consideration post-orthodontic general treatment cases (Janson, Sathler, Fernandes, Zanda, & Pinzan, 2010; Liu & Melsen, 2001), end-on Class II and full-cusp Class II were chosen as mild-Class II and severe-Class II, respectively. Skull models with Class II occlusions were created by modifying the skull with occlusion Class I. The right upper first premolar (#14) was extracted and the neighboring teeth, second premolar (#15), first molar (#16), and second molar (#17) were moved along a mesial direction to adjust molar relationships. Half of the space created by the extraction of tooth #14 remained in the case of the skull with end-on Class II occlusion, whereas in the case of the skull with full-cusp Class II occlusion, that space was filled by the neighboring teeth.

The food bolus was simplified as a rectangular parallelepiped configuration, and the size determined by considering the range of the molars to be 18 mm × 32 mm × 10 mm (width × length × height) as illustrated in Figure 2. To place the food bolus between the upper and lower dentition, the mandible was moved downward by 5 mm from its initial position. Furthermore, the food bolus was cut in the form of the occlusal surface to have perfect matches between antagonistic teeth and food surfaces. Therefore, the actual distance of the food bolus between antagonistic teeth was approximately 5–6 mm. A total

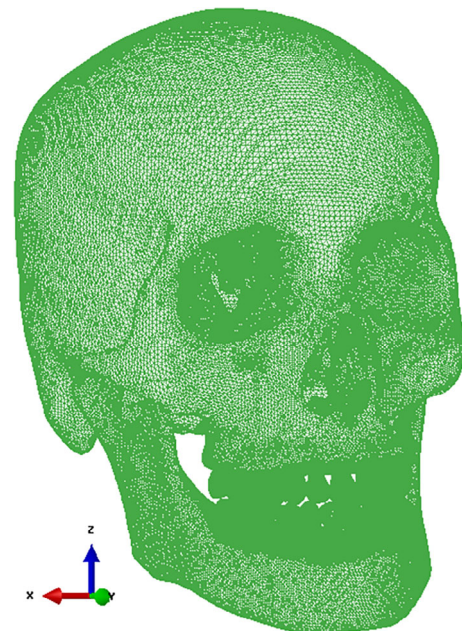


FIGURE 1 Finite element (FE) skull model with occlusion for Class I

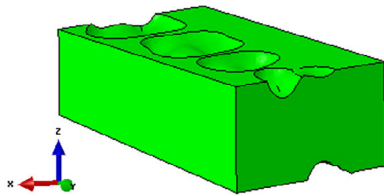
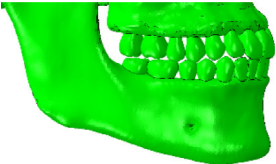
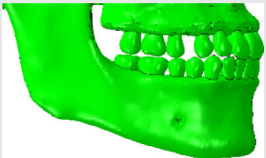
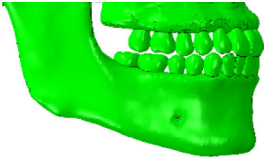
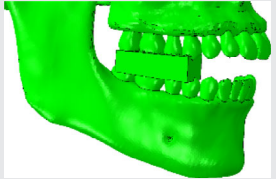
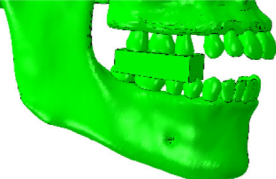
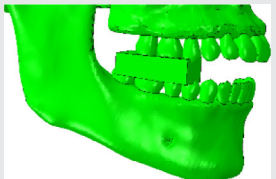


FIGURE 2 Food bolus cut in the form of the occlusal surface

TABLE 1 Details of skull models

| Model name | Occlusal relationship | Simulation | Teeth arrangement |
|------------|-----------------------|-----------------|---|
| N_NF | Class I | Teeth occluding |  |
| E_NF | End-on Class II | Teeth occluding |  |
| F_NF | Full-cusp Class II | Teeth occluding |  |
| N_IF | Class I | Food chewing |  |
| E_IF | End-on Class II | Food chewing |  |
| F_IF | Full-cusp Class II | Food chewing |  |

of six FE model cases were generated according to occlusal relationships and simulation types, as seen in Table 1.

The FE models consist of five or six parts; teeth, PDL, cortical bone, cancellous bone, the temporomandibular joint (TMJ) disc, or food bolus; Table 2 outlines element details and the corresponding material properties. Each material property was linear elastic as referred to previous papers (Minch, 2013; Santis, Ambrosio, & Licoais, 2002; Singh & Detamore, 2009). Compressive strength testing was performed with candy and carrot to define the food material model since they are similar in size to the FE food model, 15 mm × 23 mm × 6 mm (width × length × height) as shown in Figure 3. As illustrated in Figure 4, stress-strain curves were obtained from the tests and the candy's linear-elastic material behavior was applied to the food bolus.

2.2 | Simulation of chewing food

The skull models were imported into commercial software ABAQUS ver. 6.10-3 (Dassault Systemes, Velizy-Villacoublay, France) to prescribe loading and boundary conditions for chewing simulation. Small sliding contact with a friction coefficient of 0.2 (Wierszycki, Kakol, & Lodygowski, 2006) was established between the upper and lower dentition (two-body interaction) for the skull models without food; N_NF, E_NF, and F_NF. In cases of the skull including food, N_IF, E_IF, and F_IF, the surfaces between antagonistic teeth and the food bolus (three-body interaction) were simulated perfect bonding to avoid penetration error in the food model. In both the skull models with food and without food, interfaces between teeth and PDL, between PDL and bone, and between TMJ disc and bone were modeled by sharing nodes to make the connectivity of structural behaviors. In this study, it was assumed that chewing food is primarily driven by mandibular movement in a coronal-apical direction (Kim, Lee, & Park, 2016; Merdji et al., 2013) and simulated in a single cycle (Martinez Choy, Lenz, Schweizerhof, Schmitter, & Schindler, 2017). Two points were selected at the mandibular surface as loading points taking into consideration the location of the first molar and driving direction of the masseter muscle, which are the keys to masticatory activity. Loading was prescribed in the form of displacement control as the points were moved up 5 mm in the z-direction and freed in all other directions. The periphery of the foramen magnum was constrained in all translational degrees of freedom to make the skull models statically stable during loading.

3 | RESULTS

3.1 | Masticatory force-mandible movement curves

The first assessment was the relationship between masticatory force and mandible movement in the skull models; masticatory forces were calculated as the sum of reaction forces at the constrained region.

| Part | Number of elements | Size of elements | Elastic modulus | Poisson's ratio |
|-----------------|---------------------|------------------|-----------------|-----------------|
| Teeth | 569,172~587,766 | 0.2~0.7 mm | 20 GPa | 0.3 |
| PDL | 64,300~66,844 | 0.3~1.0 mm | 0.75 MPa | 0.45 |
| Cortical bone | 1,817,511~1,820,741 | 0.3~3.0 mm | 14.5 GPa | 0.323 |
| Cancellous bone | 879,726~890,403 | 0.6~2.5 mm | 1.37 GPa | 0.3 |
| TMJ disc | 1,465~1,925 | 0.8~3.0 mm | 21.7 MPa | 0.3 |
| Food (candy) | 65,161~67,783 | 0.4~1.2 mm | 120.17 MPa | 0.2 |

TABLE 2 Element details and material properties of each parts

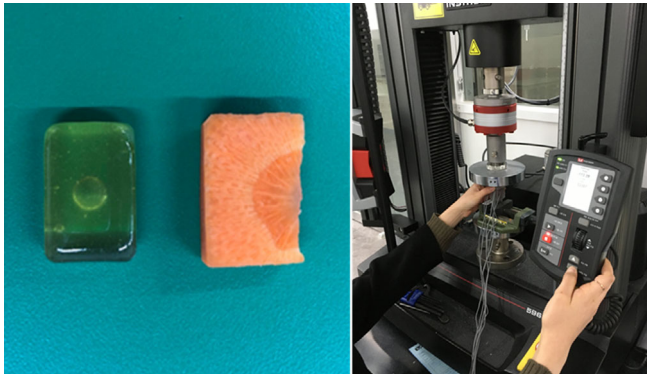


FIGURE 3 Compressive strength test setup of candy and carrot

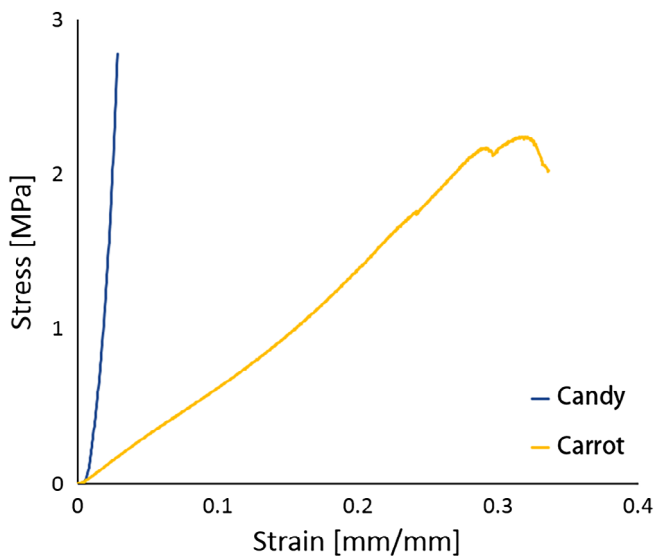


FIGURE 4 Stress-strain curves obtained from tests of food

Figure 5 shows the force-displacement curves obtained from the analytical results, and Figure 6 is a part of Figure 5 focusing on the average range of human masticatory force.

The skull models including food exhibit higher masticatory forces than the skull models without food in a very early stage of mandibular movement because the teeth in N_IF, E_IF, and F_IF were in perfect contact with the food bolus from the initial position, while there was a gap between the maxillary and mandibular teeth in N_NF, E_NF, and F_NF. Skull models without food showed several changes in the slope

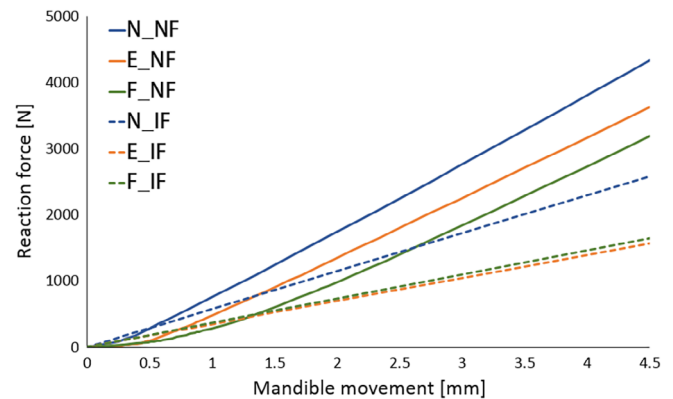


FIGURE 5 Force-displacement relationships obtained from finite element (FE) analysis

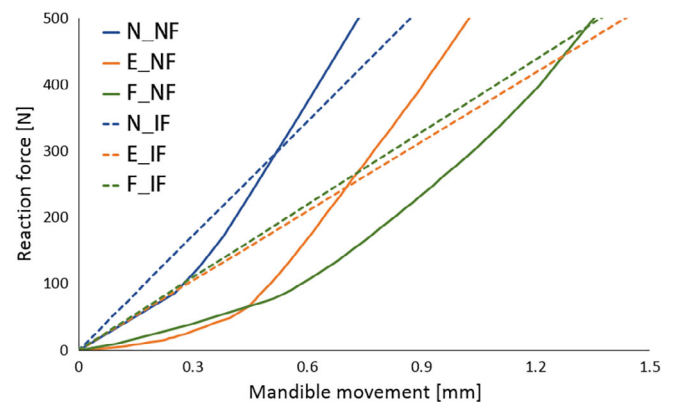


FIGURE 6 Force-displacement relationships in the range of masticatory force

of force-displacement with changes in the contact area between the teeth.

After the mandibular movement reached around 1.5 mm, the maxillary and mandibular teeth occluded adequately enough; masticatory force and the slope of the skull models without food drastically increased as shown in Figure 5. An elastic modulus of teeth (20 GPa) was greater than that of food (120.17 MPa); therefore, N_NF, E_NF, and F_NF under occluding teeth simulation showed a tendency to have higher masticatory forces than N_IF, E_IF, and F_IF

under simulation of chewing food. As a result, the curves in Figure 6 showed that there was no significant difference between skulls with food and without food in the average range of human masticatory force.

3.2 | Stress distributions

The second assessment was von Mises stress distribution of the skull. Figure 7 illustrates the stress profiles of skull models without food,

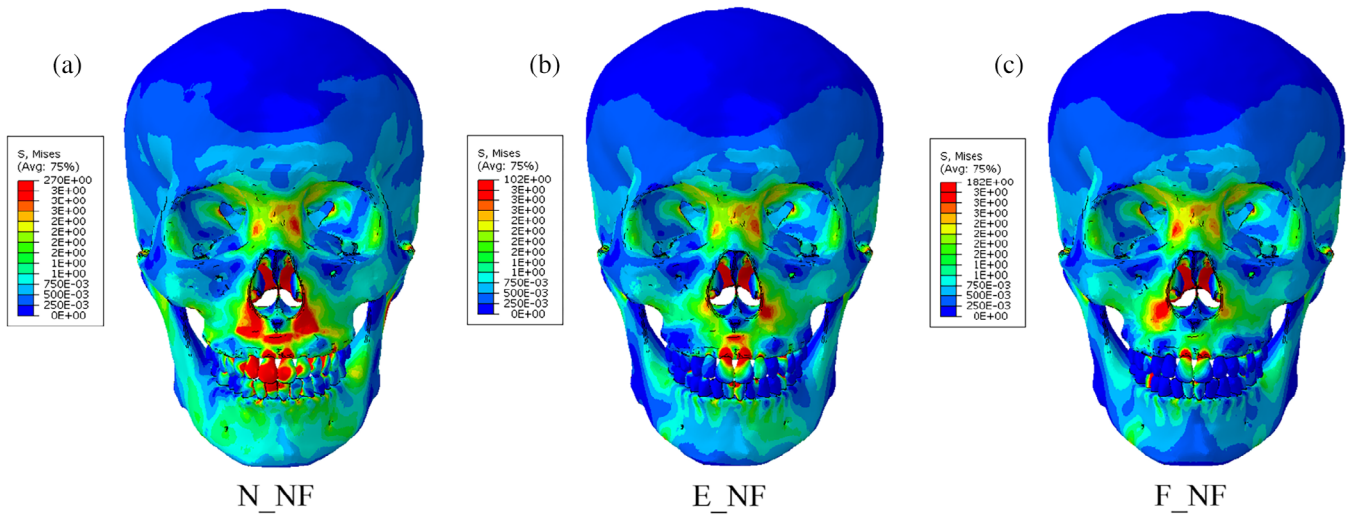


FIGURE 7 Stress distributions of the skull models without food

TABLE 3 Comparison of stresses of the skull models including food

| Model | Stress distribution | | Average stress value of roots (MPa) | | | | |
|-------|---------------------|-----------------|-------------------------------------|-----|-----|-----|-----|
| | Full skull | Molars and food | Teeth | #14 | #15 | #16 | #17 |
| N_IF | | | Teeth | #14 | #15 | #16 | #17 |
| | | | Stress | 2.0 | 1.6 | 2.4 | 1.4 |
| | | | Teeth | #44 | #45 | #46 | #47 |
| | | | Stress | 0.8 | 0.7 | 2.1 | 0.7 |
| E_IF | | | Teeth | #14 | #15 | #16 | #17 |
| | | | Stress | NA | 2.7 | 4.9 | 2.4 |
| | | | Teeth | #44 | #45 | #46 | #47 |
| | | | Stress | 0.8 | 1.0 | 2.8 | 1.0 |
| F_IF | | | Teeth | #14 | #15 | #16 | #17 |
| | | | Stress | NA | 2.6 | 4.4 | 2.2 |
| | | | Teeth | #44 | #45 | #46 | #47 |
| | | | Stress | 1.1 | 1.0 | 2.8 | 0.9 |

and Table 3 presents the stress profiles of the full skull and the molar parts including food, and the average stress values at molar roots, which are obtained from the skull models with food. The pictures were captured at an occlusal force level of about 250 N, the average human masticatory force (Kwon, Yoo, Kwon, & Kim, 2006). The stress values in Table 3 were calculated as the average of von Mises stress components at integration point of each element, which was selected in molar roots.

Stress distributions of the skulls without food generally show a comparable tendency regardless of occlusal relationships. As shown in Figure 7, relatively high stresses are observed in nasal bone and periphery of nasal cavity, and zygomatic bone and frontal bone have almost same stress profiles.

In the cases of the skulls with food (Table 3), stress propagation of the full skull was generally similar in all three cases. Stress was distributed from the loading points of the mandibular surface to the mandibular body, ramus, and condyle. Notably, it was shown that stress was concentrated in the mandibular notch, where the cranium tied with the TMJ disc, and in the alveolar bone around mandibular molars. In the maxilla, stresses were distributed in the areas of the frontal process, zygomatic bone, nasal bone, lacrimal bone, and orbital plate, but it was not significantly observed from frontal bone or the left side of the skulls. It was predicted that stresses primarily occur on the side of chewing food and propagated from the mandible to the maxilla.

The relatively high stresses were observed at tooth roots #16 and #46 in all the cases although stress concentration was different between normal occlusion; N_IF, and occlusions for Class II; E_IF and F_IF. As shown in stress distributions of the full skull, stresses observed from Class II occlusions were slightly higher at the alveolar bone around the lower first and second molars, and around maxillary molars. As shown in Table 3, the stress values at root #15~17 of E_IF (2.38807~4.91829 MPa), and F_IF (2.20813~4.39060 MPa) are much higher than that of N_IF (1.39675~2.35108 MPa). Moreover, the parts of molars including food showed that stresses were concentrated in roots #14, #16, and #46 only of N_IF, while the stresses distributed on relatively large area of all the roots (#15~17 and #44~47) of E_IF and F_IF. Since the models of E_IF and F_IF had fewer teeth to bear masticatory force than N_IF due to tooth extraction, the remained teeth in the models with Class II occlusions happened to be subjected to stresses larger than the model with normal occlusion.

4 | DISCUSSION

4.1 | Experiment for validation of the analytical methodology

In general, most analytical studies of the human body are compared to *in vivo* or *in vitro* tests for validation. However, it is difficult to ensure the safety of participants in experimental testing related to dental biomechanical research due to the limited area accessible for data measurement. In previous studies (Lee et al., 2016, 2017), replica skull specimens were fabricated based on the CT images, which were used for FE models, and occluding teeth tests were conducted. As shown in Figure 8, strain gauges were attached to selective locations on the skull and teeth, such as the buccal and palatal surface of molars, the frontozygomatic suture on the lateral orbital rim, and the zygomatic process of the temporal bone. Both experimental and FE analytical results showed a similar tendency; strains at the palatal surface of molars were the highest, while those at the buccal surface of molars were the lowest. Furthermore, strains that occurred during testing were generally 6~7 times bigger than those predicted from the FE

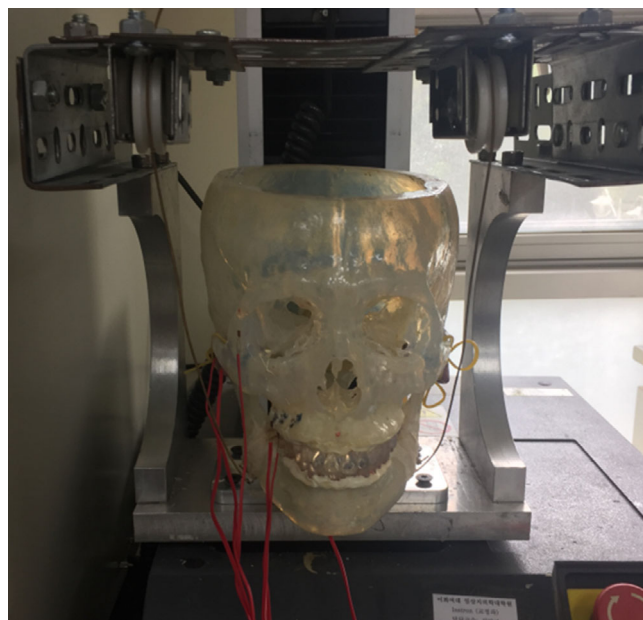


FIGURE 8 Experimental setup (Lee et al., 2017)

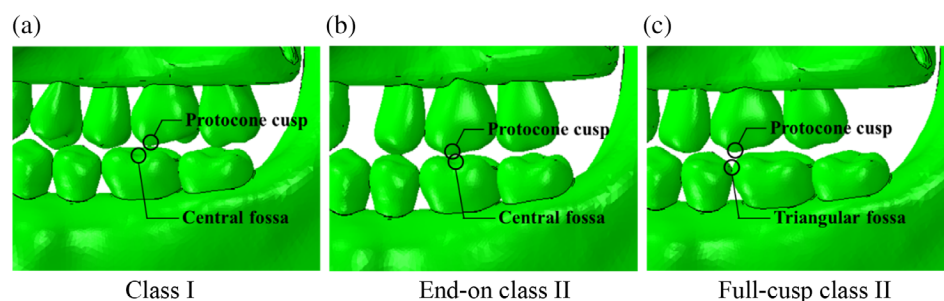


FIGURE 9 Comparison of molar relationships at the palatal side

analyses. The difference of strains is similar to the difference in material properties, because photopolymer resin (TSR-821) used for the experimental specimen has an elastic modulus of 1.8 GPa, which is around 8 times lower than material models applied to the FE analysis. Even though the FE model uses material properties simplified as linear elastic and is prescribed with translational loading direction, the experimental results are in good agreement with the analytical results taking into consideration the difference in material properties. This study uses simplified and homogenized material properties, and prescribes loading in translational direction. For the more accurate simulation of human masticatory action and the observation in microlevel, current modeling methods need to be improved by imposing composite material models and prescribing masticatory movement using masseter muscles, which are not within the scope of this study.

4.2 | Evaluation of analytical result from the clinical viewpoint

The predicted analytical results need to be reasonable from a clinical perspective related to post-orthodontic treatment cases, not only structural and mechanical viewpoints. Comparing the results among the FE models without food in Figure 5, the bite force–mandible movement curve predicted from the model of E_NF was close to the curve from N_NF, more than the curve from F_NF. In practice, the occlusal relationship of full-cusp Class II is aesthetically better since there is no embrasure between teeth. However, it is theoretically explained that occlusion for full-cusp Class II shows slightly worse masticatory function and efficiency than occlusion for end-on Class II. Jang, Kim, and Chun (2012) reported that cusp-to-central fossa relationships were observed in the majority of occlusions for Class I (89.6%) and end-on Class II (86.7%), while lingual cusp-to-mesial triangular fossa or a marginal ridge relationship was observed in full-cusp Class II occlusions. Therefore, occlusions for Class I and end-on Class II have similar mean occlusal contact areas, whereas full-cusp Class II occlusion has significantly lower values. Lee, Kim, and Chun (2015) also stated Class I molar relationship finishing exhibits a greater area of contact than full-cusp Class II finishing. As shown in Figure 9, the protocone cusp, the largest cusp of the maxillary first molar met the mesial-triangular fossa of lower first molar and the distal-triangular fossa of the lower second premolar during occluding teeth in a full-cusp Class II relationship, while it was put into the central fossa of the mandibular first molar in Class I and end-on Class II occlusions. The protocone cusp acts as a pestle and the central fossa functions as a socket. Since the triangular fossa cannot function properly as a socket due to its relatively even surface, occlusion for full-cusp Class II has smaller occlusal contact areas.

However, many dentists suggest that the difference between the cases in end-on Class II and full-cusp Class II is not significant from a clinical point of view (Koo et al., 2017). Mastication activity is divided into two phases; Phase 1 (incursive) and 2 (excursive) (Hiemae & Kay, 1972; Kay & Hiemae, 1974). Food is punctured and crushed by molar cusps in Phase 1, and the food processing is described as grinding

with an anterior-medial lower jaw movement in Phase 2. That is, chewing food occurs mainly during Phase 1. Benazzi, Kullmer, Grosse, and Weber (2011) identified the occlusal contact area in lower first molar through collision detection algorithms during occluding teeth simulations. The results show that the contact points are mostly the buccal and lingual marginal ridges in Phase 1. Therefore, it can be predicted that the marginal ridge of the molar performs a significant role during chewing food, instead of the central fossa in occluding teeth. In this study, the curves of masticatory force–mandible movement from E_IF and F_IF were approximately equal (Figures 5 and 6) and stress distribution of E_IF and F_IF, especially the parts of molars, were very similar to each other (Figure 7). Considering that chewing food is a more common behavior than occluding teeth, it is also predicted from the model that the occlusal relationships of end-on Class II and full-cusp Class II can be considered to have no difference from a clinical as well as a structural and mechanical viewpoint. Even when compared with stresses on maxillary and mandibular first molars (#16 and #46), which are primary teeth for mastication (Martinez Choy et al., 2017), relatively high stresses are observed at tooth #16 and #46 in Class I and Class II occlusions. This explains mechanically how orthodontic treatment with teeth extraction can result in similar masticatory function to the normal occlusion.

4.3 | Assessment of the effects of the material property of food

A parametric study was carried out to identify the effect of food on structural behaviors of the skull. Two types of food were selected taking into consideration the variation of elastic moduli; the original food model was candy, which had an elastic modulus of 120.17 MPa and the new food model was a carrot, which had an elastic modulus of 7.34 MPa (Figure 4). FE analyses applying each material model were performed under the same conditions.

Figure 10 illustrates the relationships between the masticatory force and mandible movement from the parametric study. Regardless of the type of food, the skull with a Class I occlusion showed the

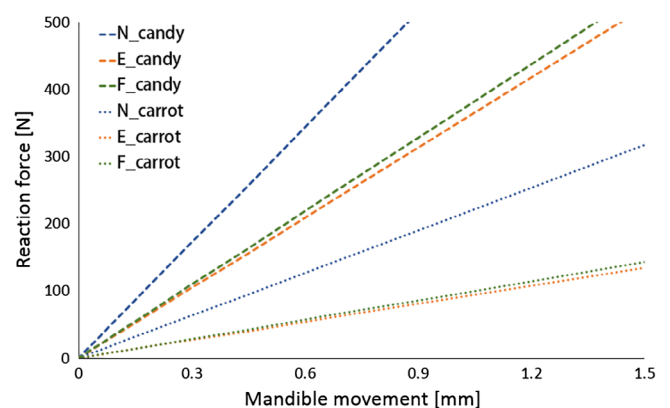


FIGURE 10 Force–displacement relationships obtained from the parametric study

highest masticatory force, followed by full-cusp Class II, and end-on Class II. According to the order of material properties, a skull chewing candy shows a greater masticatory force than a skull chewing carrot.

The elastic modulus of candy (120.7 MPa) was around 16.44 times larger than that of carrot (7.34 MPa). The slope of the curve from N_candy was approximately 2.7 times higher than that from N_carrot, and the slopes of the curves from E_candy and F_candy were about 3.8 times higher than those from E_carrot and F_carrot. Therefore, we predict that the masticatory force when chewing harder and stiffer food increases, but this increased amount is not proportional to the difference in the material properties of food.

5 | CONCLUSIONS

The relationship between masticatory force and mandible movement showed that there was no significant difference between skulls with food and without food in the range of masticatory force. In all the cases of the skull including food, stresses were similarly propagated and distributed, and the highest level of stress was observed at roots #14 and #46. Skulls with end-on Class II and full-cusp Class II occlusal relationships showed very similar masticatory forces and stress distributions, which demonstrates that the cases of end-on and full-cusp Class II can be considered to have no significant difference from clinical as well as mechanical viewpoints. The masticatory force increased when chewing harder and stiffer food comparing skulls including different food models, but the relation with differences in material properties was not linearly proportional.

REFERENCES

- Ammar, H. H., Ngan, P., Crout, R. J., Mucino, V. H., & Mukdadi, O. M. (2011). Three-dimensional modeling and finite element analysis in treatment planning for orthodontic tooth movement. *American Journal of Orthodontics and Dentofacial Orthopedics*, 139.
- Benazzi, S., Kullmer, O., Grosse, I. R., & Weber, G. W. (2011). Using occlusal wear information and finite element analysis to investigate stress distributions in human molars. *Journal of Anatomy*, 219, 259–272.
- Borcic, J., Anic, I., Smojver, I., Catic, A., Miletic, I., & Ribaric, S. P. (2005). 3D finite element model and cervical lesion formation in normal occlusion and in malocclusion. *Journal of Oral Rehabilitation*, 32, 504–510.
- Cattaneo, P. M., Dalstra, M., & Melsen, B. (2005). The finite element method: A tool to study orthodontic tooth movement. *Journal of Dental Research*, 84, 428–433.
- Chang, Y. I., Shin, S. J., & Baek, S. H. (2004). Three-dimensional finite element analysis in distal en masse movement of the maxillary dentition with the multiloop edgewise archwire. *European Journal of Orthodontics*, 26, 339–345.
- Field, C., Ichim, I., Swain, M. V., Chan, E., Darendeliler, M. A., Li, W., & Li, Q. (2009). Mechanical responses to orthodontic loading: A 3-dimensional finite element multi-tooth model. *American Journal of Orthodontics and Dentofacial Orthopedics*, 135, 174–181.
- Geramy, A., & Morgano, S. M. (2004). Finite element analysis of three designs of an implant-supported molar crown. *The Journal of Prosthetic Dentistry*, 92, 434–440.
- Hiemae, K., & Kay, R. F. (1972). Trends in the evolution of primate mastication. *Nature*, 240, 486–487.
- Hsu, M. L., Chen, C. S., Chen, B. J., Huang, H. H., & Chang, C. L. (2009). Effects of post materials and length on the stress distribution of endodontically treated maxillary central incisors: A 3D finite element analysis. *Journal of Oral Rehabilitation*, 36, 821–830.
- Jang, S. Y., Kim, M., & Chun, Y. S. (2012). Differences in molar relationships and occlusal contact areas evaluated from the buccal and lingual aspects using 3-dimensional digital models. *Korean Journal of Orthodontics*, 42, 182–189.
- Janson, G., Sathler, R., Fernandes, T. M. F., Zanda, M., & Pinzan, A. (2010). Class II malocclusion occlusal severity description. *Journal of Applied Oral Science*, 18, 397–402.
- Kay, R. F., & Hiemae, K. (1974). Jaw movement and tooth use in recent and fossil primates. *Journal of Physical Anthropology*, 40, 227–256.
- Kibi, M., Ono, T., Dong, J., Mitta, K., Gonda, T., & Maeda, Y. (2009). Development of an RPD CAD system with finite element stress analysis. *Journal of Oral Rehabilitation*, 36, 442–450.
- Kim, H. S., Lee, Y. K., & Park, J. Y. (2016). Development of FEA procedures for mechanical behaviors of maxilla, teeth and mandible. *International Journal of Precision Engineering and Manufacturing*, 17, 785–792.
- Koo, Y. J., Choi, S. H., Keum, B. T., Yu, H. S., Hwang, C. J., Melsen, B., & Lee, K. J. (2017). Maxillomandibular arch width differences at estimated centers of resistance: Comparison between normal occlusion and skeletal class III malocclusion. *Korean Journal of Orthodontics*, 47, 167–175.
- Kwon, H. K., Yoo, J. H., Kwon, Y. S., & Kim, B. I. (2006). Comparison of bite force with dental prescale and unilateral bite force recorder in healthy subjects. *The Journal of Korean Academy of Prosthodontics*, 44, 103–111.
- Lee, H., Kim, M., & Chun, Y. S. (2015). Comparison of occlusal contact areas of class I and class II molar relationships at finishing using three-dimensional digital models. *Korean Journal of Orthodontics*, 45, 113–120.
- Lee, J. S., Choi, H. I., Lee, H., Ahn, S. J., & Noh, G. (2018). Biomechanical effect of mandibular advancement device with different protrusion positions for treatment of obstructive sleep apnoea on tooth and facial bone: A finite element study. *Journal of Oral Rehabilitation*, 45, 948–958.
- Lee, Y. K., Kim, H. S., & Park, J. Y. (2017). The case study of masticatory force with food from full skull and partial model. *International Journal of Precision Engineering and Manufacturing*, 18, 1455–1462.
- Lee, Y. K., Park, J. Y., & Kim, H. S. (2016). Comparative study on structural behaviors of skull in occlusions for class I and full-cusp class II. *Journal of the Computational Structural Engineering*, 29, 309–315.
- Liang, W., Rong, Q. G., Lin, J. X., & Xud, B. H. (2009). Torque control of the maxillary incisors in lingual and labial orthodontics: A 3-dimensional finite element analysis. *American Journal of Orthodontics and Dentofacial Orthopedics*, 135, 316–322.
- Liu, D., & Melsen, B. (2001). Reappraisal of class II molar relationships diagnosed from the lingual side. *Orthodontics & Craniofacial Research*, 4, 97–104.
- Liu, T. C., Chang, C. H., Wong, T. Y., & Liu, J. K. (2012). Finite element analysis of miniscrew implants used for orthodontic anchorage. *American Journal of Orthodontics and Dentofacial Orthopedics*, 141, 468–476.
- Martinez Choy, S. E., Lenz, J., Schweizerhof, K., Schmitter, M., & Schindler, H. J. (2017). Realistic kinetic loading of the jaw system during single chewing cycles: A finite element study. *Journal of Oral Rehabilitation*, 44, 375–384.
- Merdji, A., Mootanah, R., Bouiadjra, B. A. B., Benaissa, A., Aminallah, L., Chikh, E. O., & Mukdadi, S. (2013). Stress analysis in single molar tooth. *Materials Science and Engineering C*, 33, 691–698.
- Minch, L. (2013). Material properties of periodontal ligaments. *Postępy Higieny i Medycyny Doswiadczalnej*, 67, 1261–1264.
- Rudolph, D. J., Willes, M. G., & Sameshima, G. T. (2001). A finite element model of apical force distribution from orthodontic tooth movement. *The Angle Orthodontist*, 71, 127–131.
- Santis, R. D., Ambrosio, L., & Licoais, L. (2002). Mechanical properties of tooth structures. *Integrated Biomaterials Science*, 21, 589–599.

- Seol, S. K. (2014). *Predicting of occlusal stress distribution on maxillofacial complex and skull on mastication by using finite element analysis*. Department of Medicine The Graduate School: Ewha womans University.
- Singh, M., & Detamore, M. S. (2009). Biomechanical properties of the mandibular condylar cartilage and their relevance to the TMJ disc. *Journal of Biomechanics*, 42, 405–417.
- Singh, S., Mogra, S., Shetty, V. S., Shetty, S., & Philip, P. (2012). Three-dimensional finite element analysis of strength, stability, and stress distribution in orthodontic anchorage: A conical, self-drilling miniscrew implant system. *American Journal of Orthodontics and Dentofacial Orthopedics*, 141, 327–336.
- Soares, P. V., Souza, L. V., Verissimo, C., Zeola, L. F., Pereira, A. G., Santos, P. C. F., & Fernandes-Neto, A. J. (2014). Effect of root morphology on biomechanical behaviour of premolars associated with abfraction lesions and different loading types. *Journal of Oral Rehabilitation*, 41, 108–114.
- Toms, S. R., & Eberhardt, A. W. (2003). A nonlinear finite element analysis of the periodontal ligament under orthodontic tooth loading. *American Journal of Orthodontics and Dentofacial Orthopedics*, 123, 657–665.
- Vukicevic, A. M., Zelic, K., Jovicic, G., Djuric, M., & Filipovic, N. (2015). Influence of dental restorations and mastication loadings on dentine fatigue behaviour: Image-based modelling approach. *Journal of Dentistry*, 43, 556–567.
- Wierszycki, M., Kakol, W., & Lodygowski, T. The screw loosening and fatigue analyses of three dimensional dental implant model. Paper presented at the Proceeding of 2006 ABAQUS User's Conference. 2006:527–541.
- Yu, H. S., Baik, H. S., Sung, S. J., Kim, K. D., & Cho, Y. S. (2007). Three-dimensional finite-element analysis of maxillary. *European Journal of Orthodontics*, 29, 118–125.
- Zhang, H., Cui, J. W., Lu, X. L., & Wang, M. Q. (2017). Finite element analysis on tooth and periodontal stress under simulated occlusal loads. *Journal of Oral Rehabilitation*, 44, 526–536.

SUPPORTING INFORMATION

Additional supporting information may be found online in the Supporting Information section at the end of this article.

How to cite this article: Lee Y-K, Chun Y-S. An investigation into structural behaviors of skulls chewing food in different occlusal relationships using FEM. *Clin Exp Dent Res*. 2020;6: 277–285. <https://doi.org/10.1002/cre2.273>